PRIMARY RESEARCH ARTICLE

Global Change Biology WILEY

# Dark microbial $CO_2$ fixation in temperate forest soils increases with $CO_2$ concentration

Marie Spohn[1] (iD) | Karolin Müller[2] | Carmen Höschen[3] | Carsten W. Mueller[3] | Sven Marhan[2]

[1]Soil Biogeochemistry, Bayreuth Center of Ecology and Environmental Research (BayCEER), University of Bayreuth, Bayreuth, Germany

[2]Soil Biology, Institute of Soil Science and Land Evaluation, University of Hohenheim, Stuttgart, Germany

[3]Soil Science, Technical University of Munich, Freising-Weihenstephan, Germany

**Correspondence**
Marie Spohn, University of Bayreuth, Dr. Hans-Frisch-Str. 1-3, 95448 Bayreuth, Germany.
Email: marie.spohn@uni-bayreuth.de

## Abstract

Dark, that is, nonphototrophic, microbial $CO_2$ fixation occurs in a large range of soils. However, it is still not known whether dark microbial $CO_2$ fixation substantially contributes to the C balance of soils and what factors control this process. Therefore, the objective of this study was to quantitate dark microbial $CO_2$ fixation in temperate forest soils, to determine the relationship between the soil $CO_2$ concentration and dark microbial $CO_2$ fixation, and to estimate the relative contribution of different microbial groups to dark $CO_2$ fixation. For this purpose, we conducted a $^{13}C$-$CO_2$ labeling experiment. We found that the rates of dark microbial $CO_2$ fixation were positively correlated with the $CO_2$ concentration in all soils. Dark microbial $CO_2$ fixation amounted to up to 320 µg C kg$^{-1}$ soil day$^{-1}$ in the Ah horizon. The fixation rates were 2.8–8.9 times higher in the Ah horizon than in the Bw1 horizon. Although the rates of dark microbial fixation were small compared to the respiration rate (1.2%–3.9% of the respiration rate), our findings suggest that organic matter formed by microorganisms from $CO_2$ contributes to the soil organic matter pool, especially given that microbial detritus is more stable in soil than plant detritus. Phospholipid fatty acid analyses indicated that $CO_2$ was mostly fixed by gram-positive bacteria, and not by fungi. In conclusion, our study shows that the dark microbial $CO_2$ fixation rate in temperate forest soils increases in periods of high $CO_2$ concentrations, that dark microbial $CO_2$ fixation is mostly accomplished by gram-positive bacteria, and that dark microbial $CO_2$ fixation contributes to the formation of soil organic matter.

**KEYWORDS**
anaplerotic reactions, carbon cycle, chemoautotrophic bacteria, $CO_2$ concentration, dark microbial $CO_2$ fixation, fungal–bacterial interactions, microbial carbon pump, microbial soil carbon processing, soil organic matter formation

## 1 | INTRODUCTION

Soils have mostly been studied as a source of $CO_2$ during the last decades, and organic carbon (C) in soil is assumed to have been fixed by photosynthesis (Bond-Lamberty, Bailey, Chen, Gough, & Vargas, 2018; Carey et al., 2016; Schlesinger & Andrews, 2000). However, soil microorganisms also fix $CO_2$ in the dark, and transform it into organic C (Krebs, 1941; Miltner et al., 2004, 2005; Nowak et al., 2015; Šantrůčková et al.,

2018). Yet the contribution of dark, that is, nonphototrophic, microbial $CO_2$ fixation in soils to the C cycle, and the factors that control dark microbial $CO_2$ fixation in soils are still not well understood.

It has been reported recently that dark $CO_2$ fixation rates in arctic tundra soils amounted to 0.4%–16.0% of the respiration rates (Šantrůčková et al., 2018). If dark microbial $CO_2$ fixation in soil reaches up to 16% of respiration, the process contributes substantially to C cycling in terrestrial ecosystems and needs to be taken into account for calculating soil C balances. However, currently it is difficult to estimate the importance of dark soil microbial $CO_2$ fixation for the C balance of soils, because there are only a few studies on microbial dark $CO_2$ fixation, and many of them analyzed indications of $CO_2$ fixation, such as the abundance of certain gene markers (Beulig et al., 2015; Liu et al., 2018; Yuan, Ge, Chen, O'Donnell, & Wu, 2012) or isotopic labeling of specific compounds (Ge et al., 2016), but most studies did not quantitate the proper fixation rates.

There are indications that dark soil microbial $CO_2$ fixation occurs in a large range of soils, including Mediterranean soils (Nel & Cramer, 2019), semiarid desert soils (Liu et al., 2018), arctic tundra soils (Šantrůčková et al., 2018), temperate peatland soils (Beulig et al., 2015; Nowak et al., 2015), paddy soils (Ge et al., 2016; Yuan et al., 2012), temperate meadow soils (Šantrůčková et al., 2005) as well as cropland soils (Miltner, Richnow, Kopinke, & Kästner, 2004). Thus, the process might occur ubiquitously in soils, and if quantitatively important, might affect the global C cycle. Yet, little is known about $CO_2$ fixation in temperate forest soils, and more importantly, proper $CO_2$ fixation rates have only been quantified in just a few soils so far (Miltner, Kopinke, et al., 2005; Šantrůčková et al., 2018).

Microbial fixation of $CO_2$ in the absence of light can be accomplished by a wide variety of microorganisms using different metabolic pathways. First, chemoautotrophic bacteria and archaea use $CO_2$ as the only C source (Berg et al., 2010; Saini, Kapoor, Kumar, Siddiqi, & Kumar, 2011). Second, a wide spectrum of heterotrophic bacteria and fungi employ carboxylases to replenish the citric acid cycle through anaplerotic reactions (Erb, 2011; Kornberg & Krebs, 1957). Still, little is known about the contribution of different microbial groups to dark $CO_2$ fixation in soil. Šantrůčková et al. (2018) indicated that $CO_2$ in arctic tundra soils was mostly fixed by gram-negative bacteria and to a lesser extent by gram-positive bacteria and fungi. However, aside from the evidence provided by this study, hardly anything is known about the relative contribution of bacteria and fungi to dark $CO_2$ fixation in soils.

The factors that control dark microbial $CO_2$ fixation in soil are not completely known, but there is scattered evidence that the $CO_2$ concentration might affect dark microbial $CO_2$ fixation. The $CO_2$ concentration in soils is much higher than in the atmosphere, and ranges typically between 1% and 2%, but can get as high as 13% (Amundson & Davidson, 1990). Thus, the high $CO_2$ concentration in soil might facilitate dark microbial $CO_2$ fixation. Krebs (1941) reported that heterotrophic $CO_2$-fixing propionic bacteria grew submerged in agar, where the $CO_2$ concentration was high, and only in experiments, in which the atmospheric $CO_2$ concentration was increased, they grew on the surface of the agar. More recently, Šantrůčková et al. (2005)

reported that dark microbial $CO_2$ fixation was higher in alkaline than in acid soils, and the authors explained this by the higher $HCO_3^-$ concentration in these soils. Aside from these two studies, nothing is known about the relationship between the $CO_2$ concentration and dark microbial $CO_2$ fixation, to our knowledge.

The objective of this study was (a) to quantitate dark microbial $CO_2$ fixation in three temperate forest soils that are typical for Central European forests; (b) to determine the relationship between the $CO_2$ concentration and dark microbial $CO_2$ fixation rate; and (c) to estimate the relative contributions of different microbial groups to dark $CO_2$ fixation. We hypothesized that (a) dark microbial $CO_2$ fixation in temperate forest soils contributes substantially to C cycling and the C balance of temperate forest soils; (b) the microbial $CO_2$ fixation rate increases with the $CO_2$ concentration in soil; and (c) $CO_2$ is mostly fixed by prokaryotes and not by fungi in these temperate forest soils. In order to test these hypotheses, we conducted an incubation experiment, in which we determined the dark microbial $CO_2$ fixation rate under four different $CO_2$ concentrations using $^{13}C$-$CO_2$. In addition, we estimated and visualized the contribution of different microbial groups to dark microbial $CO_2$ fixation based on phospholipid fatty acids (PLFAs) and nanoscale secondary ion mass spectrometry (NanoSIMS).

## 2 | MATERIALS AND METHODS

### 2.1 | Study sites, sampling, and sample preparation

We selected three forest sites for this study that are typical for Central Europe (Baritz, Seufert, Montanarella, & Ranst, 2010). The three sites belong to the Bavarian forestry monitoring program and the International Co-operative Programme on Assessment and Monitoring of Air Pollution Effects on Forests and have been monitored for several decades. The site Bad Brueckenau (BB) is situated in the Rhoen Mountains (50°21′N, 9°55′E) at 809 m a.s.l. and hosts a mature *Fagus sylvatica* L. forest. The mean annual rainfall amounts to 1,031 mm and the mean annual temperature is 5.8°C. The parent material is basalt, and the soil type is a dystric skeletic Cambisol (FAO). The site Mitterfels (M) is situated in the Bavarian Forest (48°53′N, 12°53′E) at 1,023 m a.s.l. and hosts a mature *F. sylvatica* L. forest. The mean annual rainfall amounts to 1,299 mm and the mean annual temperature is 4.8°C. The parent material is paragneiss, and the soil type is a hyperdystric chromic Cambisol (FAO). The site Rothenkirch (R) is situated in the Franconian Forest (50°27′N, 11°21′E) at 670 m a.s.l. and hosts a mature *Picea abies* forest. The mean annual rainfall amounts to 1,070 mm and the mean annual temperature is 6.3°C. The parent material is greywacke, and the soil type is a podzolic Cambisol (FAO). All three soils are acidic and carbonate free (Table 1). At each site, we sampled three depth increments of a soil profile, namely 0–5 cm (Ah horizon), 30–40 cm (Bw1 horizon) and 60–70 cm (Bw2 horizon) in September 2018. The soil samples were immediately transferred to the laboratory of the University of Bayreuth, where all soil samples were sieved (<2 mm) and roots were removed.

**TABLE 1** Soil chemical properties, including texture, pH, total organic carbon (TOC), and total nitrogen (TN) of the three horizons of each of the three forest soils Bad Brueckenau (BB), Mitterfels (M) and Rothenkirch (R)

| Soil | Horizon | Soil depth (cm) | Texture Sand (%) | Silt (%) | Clay (%) | $pH_{H_2O}$ | TOC (g/kg) | TN (g/kg) |
|------|---------|-----------------|-------------------|----------|----------|-------------|------------|-----------|
| BB | Ah | 0–5 | 8 | 56 | 36 | 3.9 | 159.4 | 9.7 |
| | Bw1 | 30–40 | 24 | 50 | 26 | 4.6 | 30.0 | 2.2 |
| | Bw2 | 60–70 | 29 | 51 | 20 | 5.2 | 12.2 | 1.0 |
| M | Ah | 0–5 | 48 | 33 | 20 | 3.7 | 137.3 | 7.8 |
| | Bw1 | 30–40 | 58 | 34 | 8 | 4.8 | 33.5 | 1.9 |
| | Bw2 | 60–70 | 56 | 36 | 9 | 4.9 | 17.7 | 1.1 |
| R | Ah | 0–5 | 28 | 42 | 30 | 3.9 | 79.3 | 4.5 |
| | Bw1 | 30–40 | 32 | 45 | 23 | 4.6 | 15.5 | 1.3 |
| | Bw2 | 60–70 | 40 | 43 | 17 | 4.6 | 10.5 | 1.0 |

## 2.2 | Experimental design

The rates of $CO_2$ fixation and respiration were determined in an incubation experiment at the University of Bayreuth. For this purpose, 18.0 g of each sample was weighed into incubation jars in eight replications for the Ah and Bw2 horizons, and in 20 replications for the Bw1 horizons. The incubation jars had a volume of 1,057 ml and were equipped with a septum that allowed for removal of gas samples with a syringe. Incubation jars with a large headspace volume with respect to the soil mass were chosen because we wanted the $CO_2$ concentration and its isotopic signature to change as little as possible during incubation. The water content of all samples was adjusted to 60% of their field capacity. Subsequently, we preincubated the jars at 15°C in a dark incubation chamber for 10 days. After preincubation, all jars were re-opened for several minutes to allow the $CO_2$ concentration to equilibrate with the ambient $CO_2$ concentration. Four replicates of each soil horizon were kept with air as ^{13}C natural abundance (n.a.) control treatment. In the other jars, the $CO_2$ concentration was adjusted using 99.99 at% ^{13}C-labeled $CO_2$ (Sigma-Aldrich). For this purpose, air from the closed jar was removed using a gas-tight syringe, and the same volume was replaced by pure ^{13}C-labeled $CO_2$. Four replicates of all horizons were incubated under an atmosphere of 2.50 (v/v) % $CO_2$. In addition, the Bw1 horizons of the three forest soils were incubated at 1.00, 4.70, and 6.10 (v/v) % $CO_2$, each in four replications. The reason for choosing the Bw1 horizon for the experiment with the $CO_2$ gradient is twofold; first, the $CO_2$ concentration tends to be higher in the subsoil than in the Ah horizon in many soils, second, the Bw1 horizon has a higher microbial biomass and microbial activity than the Bw2 horizon. After the $CO_2$ concentration was adjusted, all incubation jars were incubated at 15°C in the dark for 165 hr (7 days). At the very end of the incubation experiment, the jars were opened. The soil was divided, and one part of each soil sample was immediately used for the determination of microbial biomass carbon (MBC), one part was freeze dried and ground using a ball mill (Retsch GmbH), one part was frozen at −14°C for subsequent DNA and PLFA extraction, and one part was chemically fixed for NanoSIMS measurements.

## 2.3 | Respiration, microbial biomass, and DNA

The (net) respiration rate was determined based on measurements of the $CO_2$ concentrations in the glass jars performed at the beginning and at the end of the incubation experiment using a gas chromatograph (SRI 8610C; SRI Instruments Europe GmbH) equipped with a flame ionization detector. Gas samples were taken from the headspace of the jars using a syringe and then injected directly into the gas chromatograph.

In order to determine the MBC and its delta ^{13}C signature, we used the chloroform-fumigation-extraction method (Vance, Brookes, & Jenkinson, 1987). For this purpose, each soil sample was divided into two parts. One part was fumigated for 24 hr with chloroform in a desiccator before being extracted with 0.5 M $K_2SO_4$, while the other part was directly extracted in 0.5 M $K_2SO_4$. The dissolved C concentration of the extracts was determined using a total organic carbon (TOC)/TN analyzer (Multi N/C 2100S; Analytik Jena AG). The total MBC was calculated using the conversion factor of 2.22 (Joergensen, 1996). All extracts were freeze dried for isotope analysis.

DNA was extracted from 400 mg of moist soil using a DNA extraction kit (FastDNA™ SPIN Kit for Soil; MP Biomedicals) with small modifications as in Spohn, Pötsch, et al. (2016). The DNA extract was dried in silver capsules at 60°C overnight before isotope analysis.

## 2.4 | Isotope analyses

The $\delta^{13}C$ signature of the TOC, of the MBC, and of the DNA of each soil sample was determined at the Center for Stable Isotopes (KOSI) at the University of Göttingen. Samples were analyzed on a Delta V isotope ratio mass spectrometer (Thermo Fisher) interfaced to a high temperature conversion elemental analyzer Euro EA 3000 (EuroVector S.p.A).

## 2.5 | Phospholipid-derived fatty acids

Phospholipid-derived fatty acids were extracted from 2.0 g soil following the procedure described by Frostegård, Tunlid, and Bååth

(1991) with a Bligh & Dyer solution (chloroform, methanol, citrate buffer [pH 4], 1:2:0.8, [v/v/v]). Lipid fractionation and subsequent estimation of fatty acid methyl esters (FAMEs) were performed according to Kramer, Marhan, Haslwimmer, Ruess, and Kandeler (2013). For determination of the ^{13}C signature in FAMEs, an HP 6890 Gas Chromatograph (Agilent Inc.) coupled via a combustion III Interface (Thermo Finnigan) with a Delta Plus XP mass spectrometer (Thermo Finnigan MAT) was used according to the procedure described by Müller et al. (2016). In total, 30 PLFA peaks were detected with gas chromatography – flame ionization detector, but during gas chromatography combustion isotope ratio mass spectrometry analyses not all peaks were baseline separated because of either low concentration or weak separation of single fatty acids. The PLFAs i15:0, a15:0, i16:0, i17:0, and 18:1ω9 were used as biomarkers for gram-positive bacteria, cy19:0 as biomarker for gram-negative bacteria, and 18:2ω6,9 as a biomarker for fungi (Frostegård & Bååth, 1996; Frostegård, Bååth, & Tunlid, 1993; Zelles, 1999). The ^{13}C values of all FAMEs were corrected for the addition of a methyl group using a mass balance equation (Denef et al., 2007). The methanol used for methylation had a $\delta^{13}C$ value of −43.99‰.

## 2.6 | Nanoscale secondary ion mass spectrometry

Bulk soil samples were chemically fixed using Karnovsky fixative (Karnovsky, 1965) and dehydrated in graded ethanol series and dried via critical point drying (Quorum K850; Quorum Technologies Ltd). Dried samples were prepared on conductive graphene film (Plano) placed on brass stubs (10 mm diameter) suitable for scanning electron microscopy (SEM) and NanoSIMS. Briefly, 1 mg of dry soil material was placed on the graphene film, the nonsticking material was blown off using compressed clean air, yielding a layer of microaggregates, particulate organic matter and hyphae. To avoid charging, a coating with Au/Pd (ca. 5 nm for SEM, ca. 30 nm for NanoSIMS, Polaron Emitech SC7640 sputter coater) was applied prior to SEM and NanoSIMS analyses. Prior to NanoSIMS measurements, the samples were examined using SEM (Jeol 7200 F) in order to determine regions of interest for subsequent NanoSIMS measurements (Mueller et al., 2013).

The samples were examined using a Cameca NanoSIMS 50L. The $Cs^+$ primary ion beam was used, having a primary ion impact energy of 16 keV. Prior to the NanoSIMS measurement, contaminants and the Au/Pd coating layer were locally sputtered away using a high primary beam current (presputtering). During this presputtering stage, the reactive $Cs^+$ ions were implanted into the sample in order to enhance the secondary ion yields, until the secondary ions reached a steady state. Charging on mineral soil particles was additionally compensated using the electron flood gun of the NanoSIMS. The primary beam (ca. 2 pA) was focused at a lateral resolution of ca. 150 nm and was scanned over the sample, with $^{16}O^-$, $^{12}C_2^-$, $^{12}C^{13}C^-$, $^{12}C^{14}N^-$, $^{32}S^-$, $^{27}Al^{16}O^-$, and $^{56}Fe^{16}O^-$ secondary ions collected on electron multipliers with an electronic dead time fixed at 44 ns. To accurately separate mass isobars, for example, $^{13}C^{12}C^-$ and $^{12}C_2^1H^-$ at mass number 25,

a suitable mass resolution was achieved with appropriate slits and apertures (D1_3, ES_3, AS_2). The secondary ions were recorded using a dwell time of 1 ms/pixel, with 256 × 256 pixels for a 30 × 30 μm field of view with 40 planes per scan. Thus, each pixel corresponded to a size of ~117 nm × 117 nm. To localize the isotopic enrichment, we used open multi-isotope imaging mass spectrometry plugin in ImageJ and computed the $^{12}C^{13}C^-/^{12}C_2^-$ ratio, which is doubled compared to $^{13}C^-/^{12}C^-$. The n.a. at the instrument settings used translates into a ratio of 220 on the color scale used in the figures (Figure 4c,f).

## 2.7 | Calculations and statistical analyses

The isotope ratio of the MBC was calculated based on the extracts of the fumigated and the nonfumigated soil sample as follows:

$$\delta^{13}C = \frac{\left(\delta^{13}C_{fum} \times C_{fum} - \delta^{13}C_{non-fum} \times C_{non-fum}\right)}{\left(C_{fum} - C_{non-fum}\right)}. \quad (1)$$

The amount of C that was fixed in the soil and in the MBC pool was calculated from the isotope ratio of the labeled sample and the n.a. sample, as follows:

$$C \text{ fixed (mg/kg)} = \left(\frac{^{13}C}{^{12}C}\right)_{labeled} \times C \text{ (mg/kg)} - \left(\frac{^{13}C}{^{12}C}\right)_{n.a.} \times C \text{ (mg/kg)}, \quad (2)$$

where $C$ is the C concentration of the respective pool. The $^{12}C/^{13}C$ ratio was obtained from the $\delta^{13}C$ based on the $^{13}C/^{12}C$ ratio of the V-PDB standard that amounts to 0.0111802 as follows:

$$\frac{^{13}C}{^{12}C} = \left(\frac{\delta^{13}C}{1,000} + 1\right) \times 0.0111802. \quad (3)$$

The C fixation rates for the total soil pool and the MBC pool were calculated by dividing the amount of fixed C (see Equation 2) by the incubation time. The rate of $CO_2$ fixation in the microbial biomass pool was normalized by the concentration of MBC. $\delta^{13}C$ enrichments were calculated for DNA and PLFAs by subtracting the $\delta^{13}C$ value of the n.a. sample from the $\delta^{13}C$ value of the labeled sample. The respiration rate was calculated by dividing the amount of $CO_2$-C respired during the incubation by the incubation time. We plotted linear models of $CO_2$ fixation as a function of the $CO_2$ concentration and calculated Pearson correlation coefficients. Normal distribution of the $CO_2$ fixation rates, the ^{13}C enrichment of the PLFAs as well as the abundance of PLFAs was tested using the Shapiro test. Rates of $CO_2$ fixation in the soil and in the soil microbial biomass were compared separately across the three soils. This analysis was conducted separately for all Ah, Bw1, and Bw2 horizons across all three soils by one-way ANOVA followed by Tukey's post hoc test. The ^{13}C enrichment of the PLFA in the Bw1 horizons was compared separately for the three Bw1 horizons by Kruskal test followed by pairwise Wilcoxon rank sum test. In addition, the abundance of different PLFAs was compared across all three Bw1 horizons by

Kruskal test followed by pairwise Wilcoxon rank sum test. In all tests, differences with a $p < .05$ were considered as statistically significant. All analyses were conducted using R version 3.4.0 (R Core Team, 2013).

## 3 | RESULTS

The rates of dark microbial $CO_2$ fixation were highest in the Ah horizons, and reached up to 320 µg $CO_2$-C kg$^{-1}$ soil day$^{-1}$ in the Ah horizon of soil M (Figure 1A). The fixation rates were 5.8, 8.9, and 2.8 times higher in the Ah horizon than in the Bw1 horizon of soils BB, M, and R, respectively (Figure 1A). Normalized on the soil TOC concentration, the dark microbial $CO_2$ fixation rates ranged between 1.1 and 5.3 µg $CO_2$-C g$^{-1}$ TOC day$^{-1}$. The fixation rates in the MBC pool per unit MBC were significantly higher in the Bw1 horizon of soil R than in the Bw1 horizon of the other two soils (Figure 1B). In addition, the fixation rates in the MBC pool per unit MBC were also

significantly higher in the Bw2 horizon of soil R than in the Bw2 horizon of the other two soils.

The rates of dark microbial $CO_2$ fixation were positively correlated with the $CO_2$ concentration in the Bw1 horizon in all three soils ($R^2 = .79$, .87, and .87 in soil BB, M, and R, respectively, all $p < .001$; Figure 2a). The $CO_2$ fixation rates per unit soil increased by a factor of 1.74, 1.73, and 1.73 in the soil BB, M, and R, respectively, when the $CO_2$ concentration was increased from 1.0% to 6.1% $CO_2$ (Figure 2a). Similarly, the fixation rates in the MBC pool were also positively correlated with the $CO_2$ concentration in all soils (Figure 2b).

The MBC concentration was 5.8–8.3 times higher, and respiration rates were 6.7–11.5 times higher in the Ah horizon than in the Bw1 horizon in the three soils (Table 2). The respiration rates of the Bw1 horizons of all three soils were very similar (Table 2). Rates of $CO_2$ fixation amounted to 1.2%–3.9% of the respiration rates (Table 2). The percentage of the fixation rate on the
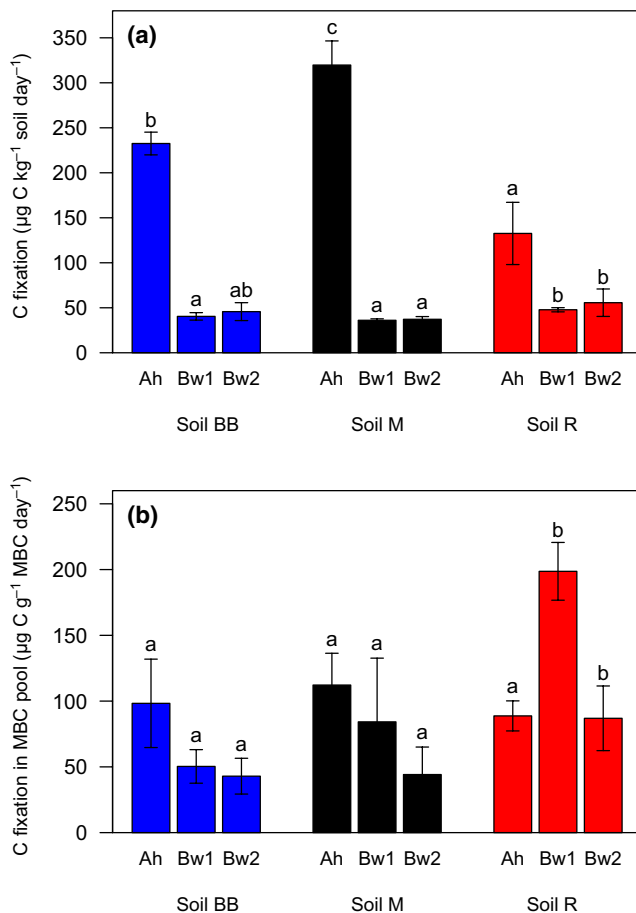


**FIGURE 1** Dark microbial $CO_2$ fixation in three horizons of the forest soils Bad Brueckenau (BB), Mitterfels (M), and Rothenkirch (R; a) in the soil and (b) in the soil microbial biomass carbon (MBC) pool determined in an atmosphere with 2.5% $CO_2$. Columns depict means ± SDs ($n = 4$). Different lowercase letters indicate significant ($p < .05$) differences tested separately for the Ah, Bw1, and Bw2 horizons across all three soils by ANOVA followed by Tukey's test
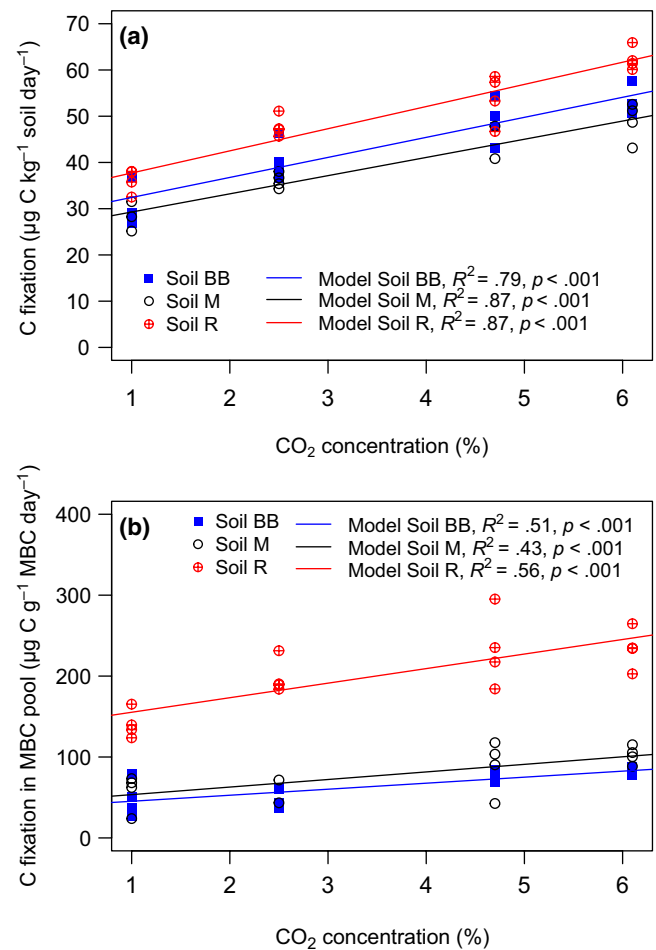


**FIGURE 2** Dark microbial $CO_2$ fixation rates as a function of the $CO_2$ concentration in the Bw1 horizon of the three forest soils Bad Brueckenau (BB), Mitterfels (M) and Rothenkirch (R; a) in the soil and (b) in the soil microbial biomass carbon (MBC) pool. Shown are four replicates per soil and $CO_2$ concentration

**TABLE 2** Soil microbial properties, including microbial biomass carbon (MBC), respiration, and dark microbial $CO_2$ fixation as percentage of respiration in three horizons of each of the three forest soils Bad Brueckenau (BB), Mitterfels (M) and Rothenkirch (R)

| Soil | Horizon | MBC (mg/kg) | Respiration (mg $CO_2$-C kg$^{-1}$ soil day$^{-1}$) | Dark $CO_2$ fixation (% of respiration) |
|---|---|---|---|---|
| BB | Ah | 1,419 ± 332 | 19.08 ± 1.11 | 1.2 ± 0.1 |
| | Bw1 | 170 ± 5 | 1.67 ± 0.13 | 2.4 ± 0.2 |
| | Bw2 | 108 ± 11 | 1.18 ± 0.29 | 3.9 ± 0.8 |
| M | Ah | 1,333 ± 64 | 13.19 ± 0.54 | 2.4 ± 0.2 |
| | Bw1 | 165 ± 23 | 1.50 ± 0.25 | 2.4 ± 0.1 |
| | Bw2 | 86 ± 9 | 0.95 ± 0.14 | 1.7 ± 2.6 |
| R | Ah | 740 ± 22 | 9.06 ± 0.60 | 1.5 ± 0.4 |
| | Bw1 | 127 ± 24 | 1.50 ± 0.25 | 2.7 ± 0.1 |
| | Bw2 | 106 ± 12 | 1.55 ± 0.02 | 3.6 ± 1.0 |

*Note:* Numbers depict means ± *SD*s (*n* = 4).

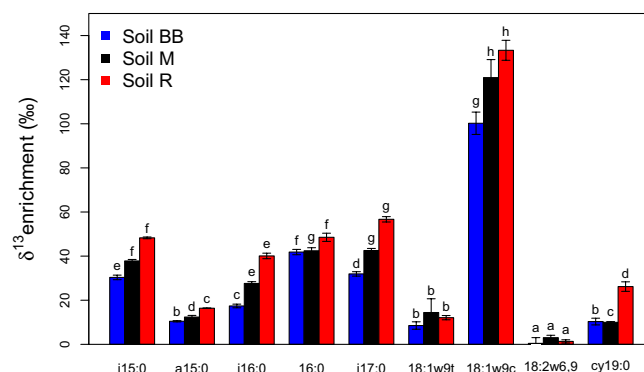**TABLE 3** $\delta^{13}$C enrichment of the total soil DNA pool in the soils Bad Brueckenau (BB), Mitterfels (M), and Rothenkirch (R) after labeling with $^{13}$C-$CO_2$ at different $CO_2$ concentrations in relation to the natural abundance samples

| $CO_2$ (%) | Soil | Horizon | $\delta^{13}$C enrichment of DNA (‰) |
|---|---|---|---|
| 2.5 | BB | Ah | 4.0 ± 2.7 |
| | | Bw1 | 1.2 ± 0.6 |
| | | Bw2 | 2.1 ± 0.8 |
| | M | Ah | 4.6 ± 3.0 |
| | | Bw1 | 1.2 ± 0.6 |
| | | Bw2 | 2.1 ± 0.4 |
| | R | Ah | 4.5 ± 3.0 |
| | | Bw1 | 1.4 ± 0.6 |
| | | Bw2 | 1.8 ± 0.9 |
| 1.0 | BB | Bw1 | 0.6 ± 0.4 |
| | M | Bw1 | 1.1 ± 0.4 |
| | R | Bw1 | 1.5 ± 0.4 |
| 4.7 | BB | Bw1 | 0.7 ± 0.4 |
| | M | Bw1 | 0.0 ± 0.3 |
| | R | Bw1 | 0.4 ± 0.4 |
| 6.1 | BB | Bw1 | 0.9 ± 0.7 |
| | M | Bw1 | 1.4 ± 0.2 |
| | R | Bw1 | 1.5 ± 0.3 |

*Note:* Numbers depict means ± *SD*s (*n* = 4).



**FIGURE 3** $\delta^{13}$C enrichment of nine phospholipid fatty acids in the Bw1 horizon of the soils Bad Brueckenau (BB), Mitterfels (M), and Rothenkirch (R) after labeling with $^{13}$C-$CO_2$ in an atmosphere with 6.1% $CO_2$ in relation to the natural abundance samples. Columns depict means ± *SD*s (*n* = 4). Different lowercase letters indicate significant (*p* < .05) differences tested separately for the three soils by Kruskal test followed by pairwise Wilcoxon rank sum test

respiration rate tended to increase with soil depth in soil BB and R (Table 2).

The DNA pool was only very weakly enriched with $^{13}$C in all three forest soils independently of the $CO_2$ concentration (Table 3). The $\delta^{13}$C enrichment of the DNA pool was higher in the Ah horizon than in the two Bw horizons in all three soils (Table 3). The $\delta^{13}$C enrichment of the PLFAs showed a consistent pattern across all three soils. The $\delta^{13}$C enrichment was significantly highest in PLFA 18:1ω9c in all three soils, reaching up to 133‰ $\delta^{13}$C (Figure 3). The PLFAs i15:0,

a15:0, i16:0, and i17:0 that are produced by gram-positive bacteria were also enriched in $^{13}$C in all three soils. The PLFA 18:2ω6,9 which is produced by fungi showed only a very low $^{13}$C enrichment in all three soils, between 0.4‰ and 3.0‰ $\delta^{13}$C. The PLFA cy19:0 that is produced by gram-negative bacteria was more weakly enriched than the PLFAs i15:0 and i17:0 that are produced by gram-positive bacteria. The $^{13}$C enrichment in 18:1ω9c as well as in i15:0, a15:0, i16:0, and i17:0 increased from soil BB, to soil M, and was highest in soil R (Figure 3). The PLFA 18:1ω9c, which was most strongly enriched in $^{13}$C, was significantly more abundant in soil R than in the other two soils (Table S1).

The NanoSIMS measurements revealed $^{13}$C-enriched micro-patches, presumably bacterial cells, in the soils that had a size of about 585 nm × 585 nm (Figure 4). The $^{13}$C-enriched cells were associated with fungal hyphae (Figure 4b), although the hyphae themselves were not enriched in $^{13}$C (Figure 4c). Furthermore, we observed that $^{13}$C-enriched micropatches were associated with particulate organic matter (Figure 4e).
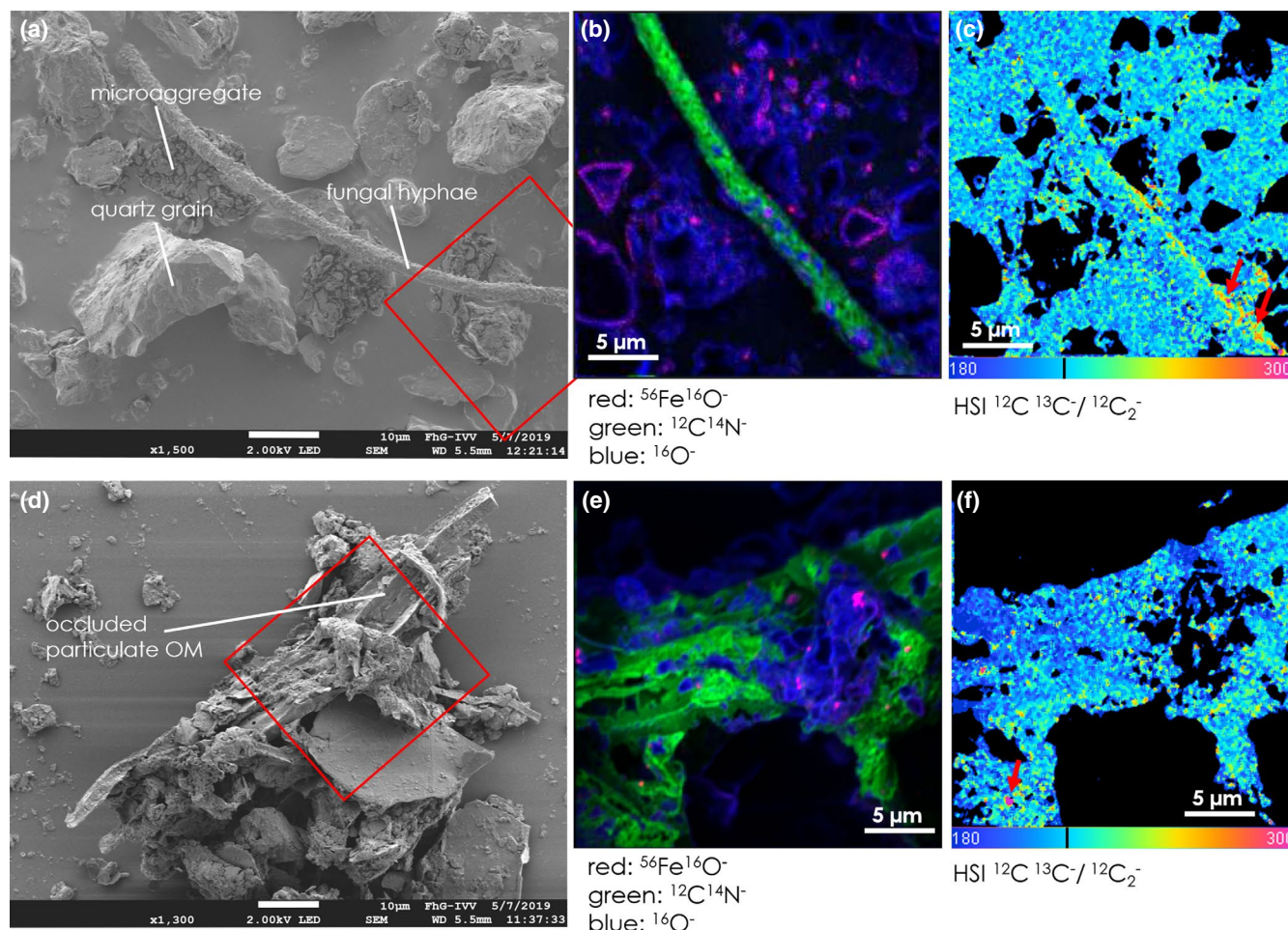
**FIGURE 4** Image analyses of locations of dark soil microbial $CO_2$ fixation, including micrographs gained by scanning electron microscope with red squares indicating area measured using NanoSIMS (a and d), composite images derived from NanoSIMS measurements showing organic matter ($^{12}C^{14}N^-$) and mineral particles ($^{16}O^-$; $^{56}Fe^{16}O^-$; b and e), and hue–saturation–intensity (HSI) maps of the ratio of $^{12}C^{13}C^-/^{12}C_2^-$, where the black line in the color bar indicates the ratio of $^{12}C^{13}C/^{12}C_2$ at natural abundance (c and f). Upper panel: (a) Microaggregates and a fungal hyphae in soil R, horizon Bw1, after labeling with $^{13}C$-$CO_2$ in an atmosphere with 6.1% $CO_2$, (b) organic matter of the fungal hyphae surrounded by mineral particles, and (c) spots of isotopic enrichment attached to the fungal hyphae (red arrows). Lower panel: (d) Microaggregate with occluded particulate organic matter (oPOM) in soil M, horizon Bw1, after labeling with $^{13}C$-$CO_2$ in an atmosphere with 6.1% $CO_2$, (e) organic carbon of the oPOM with adhering mineral particles, and (f) spots of isotopic enrichment attached to oPOM (red arrows)

## 4 | DISCUSSION

We found that the rate of dark $CO_2$ fixation was positively correlated with the $CO_2$ concentration in soils (Figure 2), which has never been described before, to our knowledge. The $CO_2$ concentration in soils is highly dynamic and can increase to up to 13% of the soil air (Amundson & Davidson, 1990). In this light, our results indicate that more $CO_2$ is fixed in soils in periods of high soil $CO_2$ concentration and in soil microsites that have a high $CO_2$ concentration. The linear relationship between the $CO_2$ concentration and the dark microbial $CO_2$ fixation rate indicates that the process is controlled by the partial pressure of $CO_2$. Reactions that lead to the fixation of $CO_2$ are carboxylation reactions that are catalyzed by carboxylases in microorganisms. Carboxylases catalyze carboxylation as well as decarboxylation of organic compounds and the equilibrium of the reaction depends on the concentrations of all compounds involved in the reaction, according to

Le Chatelier's principle. An increase in the $CO_2$ concentration moves the equilibrium of the reaction toward the product of the carboxylation reaction, and thus to an increase in $CO_2$ fixation. Our findings show that the carboxylation reaction in soil microorganisms is very sensitive to changes in the $CO_2$ concentration. We found that the $CO_2$ fixation rate and the $CO_2$ concentration were linearly correlated in the concentration range between 1.0% and 6.1% $CO_2$. It could be that at a higher $CO_2$ concentration, a saturation is reached and the fixation rate increases less with the $CO_2$ concentration than below a $CO_2$ concentration of 6.1%. However, $CO_2$ concentrations beyond 6.1% do likely not occur very frequently in many soils (Amundson & Davidson, 1990).

Our results suggest that in periods, in which large amounts of $CO_2$ are respired, a larger percentage of $CO_2$ is fixed by soil microorganisms, leading to a negative feedback of the $CO_2$ concentration on soil net $CO_2$ emission. However, it has to be taken into account that the

rates of dark microbial $CO_2$ fixation were small and only amounted to less than 4% of the net respiration rates. Hence, the negative feedback that the $CO_2$ concentration exerts on the overall soil $CO_2$ emission due to its positive effect on dark microbial $CO_2$ fixation is small.

Although the rates of dark microbial fixation in the temperate forest soils studied here were small compared to the respiration rates, our findings indicate that organic matter formed by microorganisms from $CO_2$ contributes to the soil organic matter pool. Dead microbial biomass (microbial necromass) is a very important source of soil organic matter since it is relatively stable in soil compared to plant detritus (Liang, Amelung, Lehmann, & Kästner, 2019; Miltner, Bombach, Schmidt-Brücken, & Kästner, 2012; Schimel & Schaeffer, 2012). Thus, C that enters the soil through the microbial biomass pool likely remains much longer in soil than C that enters the soil as plant detritus and mostly leaves the soil again in the form of $CO_2$ after only a few years (Sierra, Hoyt, He, & Trumbore, 2018). Hence, dark microbial $CO_2$ fixation might substantially contribute to the formation of soil organic matter in temperate forests. Furthermore, the NanoSIMS images indicate that labeled bacteria were associated with organic matter in microaggregates, which are assumed to be relatively stable in soil (Figure 4 lower panel). This finding provides additional evidence that $CO_2$ that is fixed in soils by bacteria directly enters relatively stable pools of organic matter in soil. Our results are in accordance with the emerging understanding that the microbial biomass is an important contributor of organic matter in soils (Kallenbach, Frey, & Grandy, 2016; Schimel & Schaeffer, 2012; Spohn, Klaus, Wanek, & Richter, 2016). To what extent dark microbial C fixation contributes to the formation of soil organic matter that remains in soil for a long period of time depends ultimately on the persistence of microbial necromass in soil. Thus, a full evaluation of the contribution of dark microbial $CO_2$ fixation to the formation of stable organic C in soil would require detailed information on the turnover of microbial necromass in soil.

We found that the dark microbial $CO_2$ fixation rates in relationship with the respiration rate were in a similar range as in Miltner, Kopinke, et al. (2005) who reported that dark microbial $CO_2$ fixation rates in temperate cropland soils amounted to 0.3%–1.1% of the respiration rate. Also the absolute rates in Miltner, Kopinke, et al. (2005) were similar to our study and amounted to 420 µg C kg$^{-1}$ soil day$^{-1}$. The rates found here are also in accordance with Nowak et al. (2015) who reported that dark microbial fixation rates in organic grassland soils on natural $CO_2$ vents amounted to 20–400 µg C kg$^{-1}$ soil day$^{-1}$. However, the rates of dark microbial $CO_2$ fixation found here are much smaller than the rates reported by Šantrůčková et al. (2018) for arctic permafrost soils. They found that the $CO_2$ fixation rate across all studied soils amounted to up to 14.6 µg C g$^{-1}$ TOC day$^{-1}$ (i.e. up to 16% of the respiration rate). The reason for the much larger rates of dark microbial $CO_2$ fixation measured by Šantrůčková et al. (2018) might be the very special conditions in arctic permafrost soils. Our data and the data of similar previous studies indicate that C flux calculations based on natural C isotope signatures may be misleading since microbial fixation of $CO_2$ that has the isotopic signature of atmospheric $CO_2$ strongly increases the $\delta^{13}C$ value of soil OC.

Microbial dark $CO_2$ fixation was higher in the Ah horizon than in the Bw1 horizon of all three soils (Figure 1A). This finding is in accordance with Nowak et al. (2015) and Ge et al. (2016), showing that dark microbial $CO_2$ fixation was highest in the topsoils of grasslands on natural $CO_2$ vents and in the top of paddy soils. The reason for this might be the high concentrations of microbial biomass (Table 2) and the high concentrations of TOC (Table 1) in the Ah horizons. The latter is supported by the NanoSIMS results, revealing that microbial cells that fixed $CO_2$ were associated with organic matter (Figure 4). The interpretation that microbial $CO_2$ fixation depends on organic C is in accordance with Šantrůčková et al. (2018) and Miltner, Kopinke, et al. (2005), showing that the dark $CO_2$ fixation rates increased due to organic matter addition to soils. The observation that dark $CO_2$ fixation is associated with the presence of organic C might suggest that dark microbial $CO_2$ fixation is mostly catalyzed by heterotrophic microorganisms. However, it could also be that dark microbial fixation is high in soils in the presence of large amounts of labile organic, because large amounts of labile organic matter are usually associated with high $CO_2$ production in soil. In the present experiment, the availability of organic C for microorganisms was low since root exudation and leaching of dissolved organic C from the organic layer into the mineral soil were excluded. If dark microbial C fixation is carried out mostly by heterotrophic bacteria, as discussed above, it can be expected that the fixation rates are higher if organic C availability is increased. In addition, it could also be that some microbial groups, including gram-negative ones, that are little active under starvation conditions, become more active if more organic C is available.

The PLFA analysis revealed that $CO_2$ was fixed by the same group of microorganisms in all three soils although the soils and the study sites differed in many properties including parent material, dominant tree species, soil texture, soil TOC content (Table 1), and PLFA abundance (Table S1). Our results indicate that $CO_2$ was mainly fixed by gram-positive bacteria and only to a much smaller extent by fungi and gram-negative bacteria (Figure 3). The dominant role of bacteria over fungi in dark $CO_2$ fixation is in accordance with Šantrůčková et al. (2018). However, in contrast to Šantrůčková et al. (2018), we found only a small enrichment of $^{13}C$ in the PLFA cy19:0 that is produced by gram-negative bacteria but relatively high enrichments in PLFAs that are produced by gram-positive bacteria. This difference between Šantrůčková et al. (2018) and our study can likely be attributed to the difference in soils, since they investigated arctic permafrost soils that host a different microbial community than the temperate forest soils studied here. However, both studies agree in the finding of a dominant role of bacteria over fungi in dark $CO_2$ fixation. The NanoSIMS measurements confirmed that dark microbial $CO_2$ fixation was accomplished by bacteria and not by fungi. In addition, we observed that $CO_2$-fixing bacteria were closely associated with fungal hyphae (Figure 4 upper panel). One might speculate that $CO_2$-fixing microorganisms grow preferentially on fungal hyphae because they benefit from the $CO_2$ respired by the fungus. This speculation is supported by the finding of Krebs (1941) that $CO_2$-fixing propionic bacteria grow preferentially at microsites with high $CO_2$ concentration. However, there might be other reasons why $CO_2$-fixing prokaryotes grew preferentially on fungal hyphae; they

might, for example, also benefit from water being transported along the hyphae (Guhr, Borken, Spohn, & Matzner, 2015).

We found that the DNA was much less enriched with ^{13}C than most of the PLFAs. The reason for this might be, first, that the four nucleotides that form DNA are not completely decomposed and newly synthesized in the cell but are (at least partly) re-used, in contrast to PLFAs that are newly synthesized (Nelson, Cox, & Häcker, 2009). Second, $CO_2$ fixed through anaplerotic reactions enters the microbial cell through the citric acid cycle and is incorporated into citrate, which is an important precursor of fatty acids, while the pentose that contains a large part of the C in DNA is not built up from compounds of the citric acid cycle in heterotrophic organisms (Nelson et al., 2009). Our results are in accordance with Miltner et al. (2004), observing that amino sugars were much less enriched with ^{13}C than amino acids after incubating soil from a cropland with [13]C-$CO_2$. The findings that sugar-containing compounds are less enriched in $CO_2$-derived C indicate that dark microbial $CO_2$ fixation is mostly accomplished by heterotrophic microorganisms.

Significantly more $CO_2$ was fixed in the microbial biomass in the Bw1 horizon of soil R than in the Bw1 horizon of the other two soils (Figures 1B and 2b) and also some PLFAs were more strongly enriched with ^{13}C in soil R than in the other two soils (Figure 3). This is especially noteworthy given that the respiration rates of the three Bw1 horizons were very similar (Table 2), indicating that the overall microbial activity did not differ between the three soil horizons. The reason for the significantly higher $CO_2$ fixation rate in the upper subsoil of the spruce forest soil (horizon Bw1 of soil R) might be a different microbial community that fixes more $CO_2$ compared to the corresponding horizon in the two beech forest soils. This is supported by the finding that the PLFA 18:1ω9c, which was most strongly enriched in [13]C (Figure 3) was significantly more abundant in soil R than in the other two soils (Table S1). The difference in the microbial community might be caused by the difference in forest type (beech forest at sites BB and M, and spruce forest at site R) since tree species affect the microbial community composition in temperate forest soils (Hackl, Pfeffer, Donat, Bachmann, & Zechmeister-Boltenstern, 2005).

In conclusion, our study shows that dark microbial $CO_2$ fixation rates increase linearly with the soil $CO_2$ concentration, indicating that more $CO_2$ is fixed in periods or microsites with high soil $CO_2$ concentrations. In addition, our findings show that dark $CO_2$ fixation in temperate forest soils is mostly accomplished by gram-positive bacteria and not by fungi. Although the rates of dark microbial fixation were small compared to the respiration rates, our findings suggest that organic matter formed by microorganisms from $CO_2$ contributes to the soil organic matter pool, especially given that microbial detritus is more stable in soil than plant detritus.

## ORCID

*Marie Spohn* 🆔 https://orcid.org/0000-0002-1010-7317

## REFERENCES

Amundson, R. G., & Davidson, E. A. (1990). Carbon dioxide and nitrogenous gases in the soil atmosphere. *Journal of Geochemical Exploration*, *38*(1–2), 13–41. https://doi.org/10.1016/0375-6742(90)90091-N

Baritz, R., Seufert, G., Montanarella, L., & Van Ranst, E. (2010). Carbon concentrations and stocks in forest soils of Europe. *Forest Ecology and Management*, *260*(3), 262–277. https://doi.org/10.1016/j.foreco.2010.03.025

Berg, I. A., Kockelkorn, D., Ramos-Vera, W. H., Say, R. F., Zarzycki, J., Hügler, M., ... Fuchs, G. (2010). Autotrophic carbon fixation in archaea. *Nature Reviews Microbiology*, *8*(6), 447–460. https://doi.org/10.1038/nrmicro2365

Beulig, F., Heuer, V. B., Akob, D. M., Viehweger, B., Elvert, M., Herrmann, M., ... Küsel, K. (2015). Carbon flow from volcanic $CO_2$ into soil microbial communities of a wetland mofette. *The ISME Journal*, *9*(3), 746.

Bond-Lamberty, B., Bailey, V. L., Chen, M., Gough, C. M., & Vargas, R. (2018). Globally rising soil heterotrophic respiration over recent decades. *Nature*, *560*(7716), 80–83. https://doi.org/10.1038/s41586-018-0358-x

Carey, J. C., Tang, J., Templer, P. H., Kroeger, K. D., Crowther, T. W., Burton, A. J., ... Tietema, A. (2016). Temperature response of soil respiration largely unaltered with experimental warming. *Proceedings of the National Academy of Sciences of the United States of America*, *113*(48), 13797–13802. https://doi.org/10.1073/pnas.1605365113

Denef, K., Bubenheim, H., Lenhart, K., Vermeulen, J., Van Cleemput, O., Boeckx, P., & Müller, C. (2007). Community shifts and carbon translocation within metabolically-active rhizosphere microorganisms in grasslands under elevated $CO_2$. *Biogeosciences*, *4*(5), 769–779. https://doi.org/10.5194/bg-4-769-2007

Erb, T. J. (2011). Carboxylases in natural and synthetic microbial pathways. *Applied and Environmental Microbiology*, *77*(24), 8466–8477. https://doi.org/10.1128/AEM.05702-11

Frostegård, Å., & Bååth, E. (1996). The use of phospholipid fatty acid analysis to estimate bacterial and fungal biomass in soil. *Biology and Fertility of Soils*, *22*(1–2), 59–65. https://doi.org/10.1007/BF00384433

Frostegård, Å., Bååth, E., & Tunlid, A. (1993). Shifts in the structure of soil microbial communities in limed forests as revealed by phospholipid fatty acid analysis. *Soil Biology and Biochemistry*, *25*(6), 723–730. https://doi.org/10.1016/0038-0717(93)90113-P

Frostegård, Å., Tunlid, A., & Bååth, E. (1991). Microbial biomass measured as total lipid phosphate in soils of different organic content. *Journal of Microbiological Methods*, *14*(3), 151–163. https://doi.org/10.1016/0167-7012(91)90018-L

Ge, T., Wu, X., Liu, Q., Zhu, Z., Yuan, H., Wang, W., ... Wu, J. (2016). Effect of simulated tillage on microbial autotrophic $CO_2$ fixation in paddy and upland soils. *Scientific Reports*, *6*, 19784. https://doi.org/10.1038/srep19784

Guhr, A., Borken, W., Spohn, M., & Matzner, E. (2015). Redistribution of soil water by a saprotrophic fungus enhances carbon mineralization. *Proceedings of the National Academy of Sciences of the United States of America*, *112*(47), 14647–14651. https://doi.org/10.1073/pnas.1514435112

Hackl, E., Pfeffer, M., Donat, C., Bachmann, G., & Zechmeister-Boltenstern, S. (2005). Composition of the microbial communities in the mineral soil under different types of natural forest. *Soil Biology and Biochemistry*, *37*(4), 661–671. https://doi.org/10.1016/j.soilbio.2004.08.023

Joergensen, R. G. (1996). The fumigation-extraction method to estimate soil microbial biomass: Calibration of the kEC value. *Soil Biology and Biochemistry*, *28*(1), 25–31. https://doi.org/10.1016/0038-0717(95)00102-6

Kallenbach, C. M., Frey, S. D., & Grandy, A. S. (2016). Direct evidence for microbial-derived soil organic matter formation and its ecophysiological controls. *Nature Communications*, *7*, 13630. https://doi.org/10.1038/ncomms13630

Karnovsky, M. J. (1965). A formaldehyde-glutaraldehyde fixative of high osmolality for use in electron microscopy. *Journal of Cell Biology*, *27*(2), 137–138.

Kornberg, H. L., & Krebs, E. H. (1957). Synthesis of cell constituents from $C_2$-units by a modified tricarboxylic acid cycle. *Nature*, *179*(4568), 988–991. https://doi.org/10.1038/179988a0

Kramer, S., Marhan, S., Haslwimmer, H., Ruess, L., & Kandeler, E. (2013). Temporal variation in surface and subsoil abundance and function of the soil microbial community in an arable soil. *Soil Biology and Biochemistry*, *61*, 76–85. https://doi.org/10.1016/j.soilbio.2013.02.006

Krebs, H. A. (1941). Carbon dioxide assimilation in heterotrophic organisms. *Nature*, *147*(3732), 560–563. https://doi.org/10.1038/147560a0

Liang, C., Amelung, W., Lehmann, J., & Kästner, M. (2019). Quantitative assessment of microbial necromass contribution to soil organic matter. *Global Change Biology*, *25*(11), 3578–3590. https://doi.org/10.1111/gcb.14781

Liu, Z., Sun, Y., Zhang, Y., Feng, W., Lai, Z., Fa, K., & Qin, S. (2018). Metagenomic and $^{13}C$ tracing evidence for autotrophic atmospheric carbon absorption in a semiarid desert. *Soil Biology and Biochemistry*, *125*, 156–166. https://doi.org/10.1016/j.soilbio.2018.07.012

Miltner, A., Bombach, P., Schmidt-Brücken, B., & Kästner, M. (2012). SOM genesis: Microbial biomass as a significant source. *Biogeochemistry*, *111*(1–3), 41–55. https://doi.org/10.1007/s10533-011-9658-z

Miltner, A., Kopinke, F. D., Kindler, R., Selesi, D., Hartmann, A., & Kästner, M. (2005). Non-phototrophic $CO_2$ fixation by soil microorganisms. *Plant and Soil*, *269*(1–2), 193–203. https://doi.org/10.1007/s11104-004-0483-1

Miltner, A., Richnow, H. H., Kopinke, F. D., & Kästner, M. (2004). Assimilation of $CO_2$ by soil microorganisms and transformation into soil organic matter. *Organic Geochemistry*, *35*(9), 1015–1024. https://doi.org/10.1016/j.orggeochem.2004.05.001

Miltner, A., Richnow, H. H., Kopinke, F. D., & Kästner, M. (2005). Incorporation of carbon originating from $CO_2$ into different compounds of soil microbial biomass and soil organic matter. *Isotopes in Environmental and Health Studies*, *41*(2), 135–140. https://doi.org/10.1080/10256010412331314265

Mueller, C. W., Weber, P. K., Kilburn, M. R., Hoeschen, C., Kleber, M., & Pett-Ridge, J. (2013). Advances in the analysis of biogeochemical interfaces: NanoSIMS to investigate soil microenvironments. *Advances in Agronomy*, *121*, 1–46. https://doi.org/10.1016/B978-0-12-407685-3.00001-3

Müller, K., Kramer, S., Haslwimmer, H., Marhan, S., Scheunemann, N., Butenschön, O., ... Kandeler, E. (2016). Carbon transfer from maize roots and litter into bacteria and fungi depends on soil depth and time. *Soil Biology and Biochemistry*, *93*, 79–89. https://doi.org/10.1016/j.soilbio.2015.10.015

Nel, J. A., & Cramer, M. D. (2019). Soil microbial anaplerotic $CO_2$ fixation in temperate soils. *Geoderma*, *335*, 170–178. https://doi.org/10.1016/j.geoderma.2018.08.014

Nelson, D. L., Cox, M. M., & Häcker, B. (2009). *Lehninger Biochemie*. Berlin and Heidelberg, Germany: Springer.

Nowak, M., Beulig, F., von Fischer, J., Muhr, J., Küsel, K., & Trumbore, S. E. (2015). Autotrophic fixation of geogenic $CO_2$ by microorganisms contributes to soil organic matter formation and alters isotope signatures in a wetland mofette. *Biogeosciences*, *12*(3), 7169–7183. https://doi.org/10.5194/bg-12-7169-2015

R Core Team. (2013). *A language and environment for statistical computing*. Vienna, Austria: R Foundation for Statistical Computing.

Saini, R., Kapoor, R., Kumar, R., Siddiqi, T. O., & Kumar, A. (2011). $CO_2$ utilizing microbes – A comprehensive review. *Biotechnology Advances*, *29*(6), 949–960. https://doi.org/10.1016/j.biotechadv.2011.08.009

Šantrůčková, H., Bird, M. I., Elhottova, D., Novak, J., Picek, T., Šimek, M., & Tykva, R. (2005). Heterotrophic fixation of $CO_2$ in soil. *Microbial Ecology*, *49*(2), 218–225. https://doi.org/10.1007/s00248-004-0164-x

Šantrůčková, H., Kotas, P., Bárta, J., Urich, T., Čapek, P., Palmtag, J., ... Richter, A. (2018). Significance of dark $CO_2$ fixation in arctic soils. *Soil Biology and Biochemistry*, *119*, 11–21. https://doi.org/10.1016/j.soilbio.2017.12.021

Schimel, J., & Schaeffer, S. M. (2012). Microbial control over carbon cycling in soil. *Frontiers in Microbiology*, *3*, 348. https://doi.org/10.3389/fmicb.2012.00348

Schlesinger, W. H., & Andrews, J. A. (2000). Soil respiration and the global carbon cycle. *Biogeochemistry*, *48*(1), 7–20. https://doi.org/10.1023/a:1006247623877

Sierra, C. A., Hoyt, A. M., He, Y., & Trumbore, S. E. (2018). Soil organic matter persistence as a stochastic process: Age and transit time distributions of carbon in soils. *Global Biogeochemical Cycles*, *32*(10), 1574–1588. https://doi.org/10.1029/2018GB005950

Spohn, M., Klaus, K., Wanek, W., & Richter, A. (2016). Microbial carbon use efficiency and biomass turnover times depending on soil depth – Implications for carbon cycling. *Soil Biology and Biochemistry*, *96*, 74–81. https://doi.org/10.1016/j.soilbio.2016.01.016

Spohn, M., Pötsch, E. M., Eichorst, S. A., Woebken, D., Wanek, W., & Richter, A. (2016). Soil microbial carbon use efficiency and biomass turnover in a long-term fertilization experiment in a temperate grassland. *Soil Biology and Biochemistry*, *97*, 168–175. https://doi.org/10.1016/j.soilbio.2016.03.008

Vance, E. D., Brookes, P. C., & Jenkinson, D. S. (1987). An extraction method for measuring soil microbial biomass C. *Soil Biology and Biochemistry*, *19*(6), 703–707. https://doi.org/10.1016/0038-0717(87)90052-6

Yuan, H., Ge, T., Chen, C., O'Donnell, A. G., & Wu, J. (2012). Microbial autotrophy plays a significant role in the sequestration of soil carbon. *Applied and Environmental Microbiology*, *78*, 2328–2336. https://doi.org/10.1128/aem.06881-11

Zelles, L. (1999). Fatty acid patterns of phospholipids and lipopolysaccharides in the characterisation of microbial communities in soil: A review. *Biology and Fertility of Soils*, *29*(2), 111–129. https://doi.org/10.1007/s003740050533

## SUPPORTING INFORMATION

Additional supporting information may be found online in the Supporting Information section.